Toxicology Research

PAPER

View Article Online
View Journal | View Issue

Cite this: *Toxicol. Res.*, 2019, **8**, 885

Ex vivo toxicological evaluation of experimental anticancer gold(I) complexes with lansoprazole-type ligands†

Natalia Estrada-Ortiz,[a] Elena Lopez-Gonzales,[a] Ben Woods,[b] Stefan Stürup,[c] Inge A. M. de Graaf,[a] Geny M. M. Groothuis *[a] and Angela Casini *[a,b,d]

Gold-based compounds are of great interest in the field of medicinal chemistry as novel therapeutic (anticancer) agents due to their peculiar reactivity and mechanisms of action with respect to organic drugs. Despite their promising pharmacological properties, the possible toxic effects of gold compounds need to be carefully evaluated in order to optimize their design and applicability. This study reports on the potential toxicity of three experimental gold-based anticancer compounds featuring lansoprazole ligands (**1–3**) studied in an *ex vivo* model, using rat precision cut kidney and liver slices (PCKS and PCLS, respectively). The results showed a different toxicity profile for the tested compounds, with the neutral complex **2** being the least toxic, even less toxic than cisplatin, followed by the cationic complex **1**. The dinuclear cationic gold complex **3** was the most toxic in both liver and kidney slices. This result correlated with the metal uptake of the different compounds assessed by ICP-MS, where complex **3** showed the highest accumulation of gold in liver and kidney slices. Interestingly compound **1** showed the highest selectivity towards cancer cells compared to the healthy tissues. Histomorphology evaluation showed a similar pattern for all three Au(I) complexes, where the distal tubular cells suffered the most extensive damage, in contrast to the damage in the proximal tubules induced by cisplatin. The binding of representative gold compounds with the model ubiquitin was also studied by ESI-MS, showing that after 24 h incubation only 'naked' Au ions were bound to the protein following ligands' loss. The mRNA expression of stress response genes appeared to be similar for both evaluated organs, suggesting oxidative stress as the possible mechanism of toxicity. The obtained results open new perspectives towards the design and testing of bifunctional gold complexes with chemotherapeutic applications.

Received 18th June 2019,
Accepted 19th September 2019

DOI: 10.1039/c9tx00149b

rsc.li/toxicology-research

Introduction

In the drug development process, it is crucial to anticipate possible side effects and predict toxicity before starting clinical trials of potential drug-like compounds not only in animal experiments but also in human-derived *in vitro* models. 2D-single-cell models are by far the most commonly used models to predict efficacy and toxicity in humans. The advantage of these models is the variety of cell types available to study, including primary cells, stem cells and cancer cells. The main disadvantage is the absence of the complexity of a tissue, with its multitude of cell types playing different roles and secreting different signaling molecules, and the absence of a proper extra cellular matrix to maintain and regulate the function and activities of the specific tissue.[1] Therefore, animal models are widely used, where the complexity of a whole organism is intact. However, the use of animals for pre-clinical studies exposes two important problems: the large number and high discomfort of sacrificed animals used bring about ethical objections and the translation of such studies from any species (even primates) to the humans is not always accurate and presents a risk to patients in the first phases of clinical trials.[2–5]

In the past decades, the technique known as precision cut tissue slices (PCTS) became a powerful technology, which can be applied to many organs.[6–10] PCTS contain all cell types of the tissue in their natural environment, with intercellular and

[a]*Dept. Pharmacokinetics, Toxicology and Targeting, Groningen Research Institute of Pharmacy, University of Groningen, A. Deusinglaan 1, 9713AV Groningen, The Netherlands. E-mail: g.m.m.groothuis@rug.nl, angela.casini@tum.de*
[b]*School of Chemistry, Cardiff University, Main Building, Park Place, CF10 3AT Cardiff, UK*
[c]*Dept. of Pharmacy, University of Copenhagen, Universitetsparken 2, 2100 Copenhagen, Denmark*
[d]*Department of Chemistry, Technical University of Munich, Lichtenbergstr. 4, 85748 Garching b. München, Germany*
†Electronic supplementary information (ESI) available. See DOI: 10.1039/c9tx00149b

cell–matrix interactions remaining intact, making the technique an ideal *ex vivo* model for human diseases, such as fibrosis and cirrhosis.[11–14] Additionally, the PCTS technique offers the opportunity to test the activity, metabolism, transport and toxicity of new drug candidates, including comparison between species and organs.[6–11,14–17] PCTS is an FDA-approved model for drug toxicity and metabolism studies and offers an opportunity of reducing the number of animals used in pre-clinical studies.[6,7,10] Using PCTS it is possible to obtain valuable knowledge on the structure–toxicity relationship of experimental compounds, enabling further optimization and selection of better candidates with improved properties and reduced toxicity in healthy tissue. Recently, we have successfully used PCTS to study the toxic effects of experimental anticancer organometallic compounds,[18–22] aminoferrocene-containing pro-drugs,[23] ruthenium-based kinase inhibitors,[24] as well as supramolecular metallacages as drug delivery systems.[15,25]

Here, we applied the PCTS technology to study the toxicity of three bifunctional metallodrugs, containing gold(I) ions complexed with a lansoprazole moiety (Fig. 1), in healthy rat liver and kidney slices, which are the most sensitive to drug-induced injury. In a previous study, the three compounds were studied for their anticancer effects in human cancer cells *in vitro*, showing promising activity profiles against cisplatin resistant human A2780 ovarian cancer cells.[26]

Following the clinical success of the Pt(II) complex cisplatin (Fig. 1) a large number of metal-containing compounds were developed with interesting cytotoxic activities and pharmacological profiles.[27–33] Among them, gold-based complexes occupy a relevant family, due to their different possible oxidation states (*e.g.* Au(I) and Au(III)), stability and ligand exchange reactions, conferring them different mechanisms of action compared to cisplatin.[32,34,35] As an example, the Au(I) complex auranofin (Fig. 1) is in clinical trials at present for the treatment of different cancers.[34,36]

Lansoprazole is a drug currently in use for the treatment of ulcers and gastroesophageal reflux disease.[37,38] The postulated mechanism of action is to selectively inhibit the membrane enzyme H^+/K^+ ATPase in gastric parietal cells.[37,39] This H^+/K^+ ATPase is a proton pump located among others in the apical membrane of parietal cells and is responsible for gastric acid secretion. Proton pump inhibitors (PPIs) exert their effects by blocking the translocation of H^+ into the stomach content thereby preventing acid formation and increasing the pH in the stomach.[37,40]

Proton pumps are also found in other cell types, such as cancer cells.[41] Thus, it has been proposed that PPIs, such as lansoprazole, can modify the acidic microenvironment present in most solid tumours and help to sensitize them to cytotoxic anticancer drugs.[39,42–44]

Within this context, in the last decade, several studies have shown a potential application in cancer research for the use of proton pump inhibitors to revert chemoresistance and increase chemosensitivity of different human tumour cells for several cytotoxic drugs.[26,45]

In the present study, we have evaluated the experimental anticancer Au(I) complexes featuring lansoprazole ligands for their toxicity in the PCTS model. These studies are necessary to assess the compounds' potential as drug candidates for further preclinical investigation. Specifically, determination of the ATP content and histomorphological studies were conducted on PCTS from rat liver and kidney treated with the Au(I) complexes in comparison to lansoprazole, cisplatin and auranofin. In addition, the relationship between toxicity and metal accumulation in the tissue slices was determined using inductively coupled plasma mass spectrometry (ICP-MS). Moreover, the reactivity of two of the gold compounds with the model protein ubiquitin was studied by electrospray ionization mass spectrometry (ESI-MS) in aqueous environment. Finally, to get more insight into the possible mechanism of toxicological action, the mRNA expression of specific stress markers in liver and kidney slices was assessed, including expression of genes coding for proteins that play important roles in the pathways of oxidative stress, apoptosis and hypoxia.

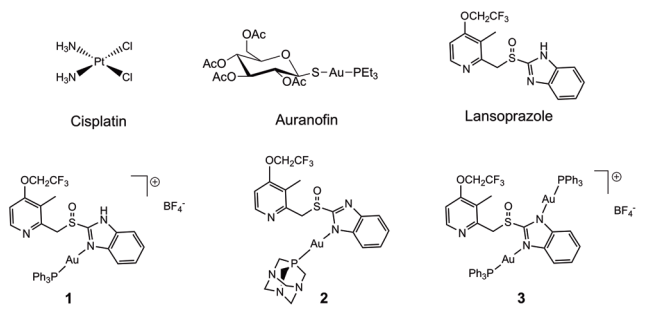

Fig. 1 Compounds evaluated in this study.

Experimental

Synthesis of the Au(I) complexes

The gold compounds **1–3** were prepared according to previously published procedures[26] and their identity and purity (≥95%) were unambiguously established using NMR spectroscopy and elemental analysis (see ESI† for details). Auranofin was purchased from Alfa-Aesar and cisplatin from Sigma-Aldrich.

Preparation of rat precision-cut liver and kidney slices (PCLS, PCKS)

Male Wistar rats (Charles River, France) of 250–300 g were housed under a 12 h dark/light cycle at constant humidity and temperature. Animals were permitted *ad libitum* access to tap water and standard lab chow. All experiments were approved by the committee for care and use of laboratory animals of the University of Groningen and the study complies with the ARRIVE guidelines and was carried out in accordance with the EU directive 2010/63/EU for animal experiments.

Kidneys and livers were harvested from the same rats (anesthetized with isoflurane) and immediately placed in University of Wisconsin solution (UW, ViaSpan, 4 °C) until

further use. After removing fat, kidneys were cut in half lengthwise using a scalpel, and cortex cores of 5 mm diameter were made from each half perpendicular to the cut surface using disposable Biopsy Punches (KAI medical, Japan). Whereas, the liver cores were prepared by using a hollow drill bit. PCKS and PCLS were made as described by de Graaf *et al.*[6,7] The cores were sliced with a Krumdieck tissue slicer (Alabama R&D, Munford, AL, USA) in ice-cold Krebs-Henseleit buffer, pH 7.4 saturated with carbogen (95% O_2 and 5% CO_2).

Liver slices (*ca.* 5 mg, ~250 μm thickness) and kidney slices (*ca.* 3 mg, ~150 μm thickness), were incubated individually in 12-well plates (Greiner bio-one GmbH, Frickenhausen, Austria), at 37 °C in 1.3 mL Williams' medium E (WME, Gibco by Life Technologies, UK) with glutamax-1, supplemented with 25 mM D-glucose (Gibco) and streptomycin (Gibco) (PCLS) ciprofloxacin HCl (PCKS) (10 μg mL^{-1}, Sigma-Aldrich, Steinheim, Germany) in an incubator (Panasonic biomedical) in an atmosphere of 80% O_2 and 5% CO_2 with shaking (90 times min^{-1}). Slices were pre-incubated 1 h and then transferred to plates with fresh medium with the tested compounds to remove debris and dead cells. Stock solutions of complexes **1** to **3**, auranofin and cisplatin were prepared by diluting a stock solution (10^{-2} M in DMSO or ethanol in the case of auranofin; 10^{-3} M in water for cisplatin). The final concentration of DMSO and ethanol during the PCLS and PCKS incubation was always below 1 and 0.025%, respectively to exclude solvent toxicity. For each treatment, three slices were incubated individually for 24 h.

Viability and TC_{50} determination

After the incubation, slices were collected for ATP and protein determination, by snap freezing them in 1 ml of ethanol (70% v/v) containing 2 mM EDTA with pH = 10.9. After thawing the slices were homogenized using a mini bead beater and centrifuged. The supernatant was used for the ATP essay and the pellet was dissolved in 5 N NaOH for the protein essay. The viability of PCKS was determined by measuring the ATP using the ATP Bioluminescence Assay kit CLS II (Roche, Mannheim, Germany) as described previously.[7] The ATP content was corrected by the protein amount of each slice and expressed as pmol μg^{-1} protein. The protein content of the PCKS was determined by the Bio-Rad DC Protein Assay (Bio-Rad, Munich, Germany) using bovine serum albumin (BSA, Sigma-Aldrich, Steinheim, Germany) for the calibration curve. The TC_{50} value was calculated as the concentration reducing the viability of the slices by 50%, in terms of ATP content corrected by the protein amount of each slice and relative to the slices without any treatment using a nonlinear fitting of log(concentration compound) *vs.* response and is presented as a mean (±SD) of at least three independent experiments.

Inductively coupled plasma mass spectrometry (ICP-MS)

After incubation for 24 h with concentrations of 5 and 10 μM of complexes **1**, **2** and cisplatin, 1 and 5 μM of complex **3**, PCKS and PCLS were snap-frozen and stored at −80 °C until the analysis.

Sample preparation

The tissue samples (triplicate slices combined) were digested with 100 μL concentrated nitric acid overnight, resulting in complete dissolution of all samples. 100 μL concentrated hydrochloric acid and 800 μL milliQ were added to produce a volume of 100 mL. Prior to analysis the samples were diluted 20 times with 0.56% HNO_3/0.1% HCl.

ICP-MS analysis

The Au and Pt contents were quantified applying a PerkinElmer (Waltham, MA, USA) Sciex Elan 6100 DRC-e ICP-MS instrument, equipped with a Cetac ASX-110FR autosampler, a 0.2 mL min^{-1} MicroMist U-series pneumatic concentric nebulizer (Glass Expansion, West Melbourne Vic, Australia) and a PC3 cyclonic spray chamber (Elemental Scientific Inc., Omaha, NE, USA). ICP-MS RF power, lens voltage and nebulizer gas and flow were optimized on a daily basis and other settings were: 1 sweep/reading, 25 readings/replicate, 5 replicates, 50 ms dwell time. $^{197}Au^+$, $^{195}Pt^+$, and $^{194}Pt^+$ isotopes were monitored. Pt and Au concentrations were determined by external calibration (0–20 ppb Pt and Au). LODs were 0.1 and 0.2 μg L^{-1} for Pt and Au, (3 × SD on blank, $n = 10$) and the spike recovery were 102% and 99% for Pt and Au, respectively. Pt and Au single element PlasmaCAL standards (SCP Science, Quebec, Canada) were used and the standards were prepared in a mixture of 0.1% HCl and 0.65% subboiled HNO_3 in MilliQ water. This mixture was furthermore used to dilute samples after digestion and as blank solution.

Histomorphology

After 24 h incubation with 25 μM for complexes **1**, **2** and cisplatin, 10 μM for complex **3** and 5 μM for auranofin, kidney slices were fixated in 4% formalin for 24 hours and stored in 70% ethanol at 4 °C until processing for morphology studies. After dehydration, the slices were embedded in paraffin and 4 μm sections were made, which were mounted on glass slides and H&E and PAS staining were used for histopathological evaluation. First, the sections were deparaffinised with xylene and ethanol 100%. For the H&E staining the glass slides were hydrated in 50% ethanol, followed by hematoxylin staining for 5 minutes, then rinsed with tap water and washed with 50% acidic ethanol (1% HCl aqueous solution) and 80% alkaline ethanol (0.02% NH_3 aqueous solution), and subsequently the sections were stained with eosin for 2 minutes and washed with ethanol 100% and xylene. For the PAS staining the sections were washed with distilled water, followed by treatment with a 1% aqueous solution of periodic acid for 20 minutes and Schiff reagent for 20 minutes, the slides were rinsed with tap water, and finally a counterstain with hematoxylin for 5 minutes was used to visualize the nuclei.

Determination of stress markers mRNA expression

RNA isolation. Three precision cut kidney and liver slices from each treatment group were snap-frozen in RNase free Eppendorf's. RNA was isolated with the Maxwell® 16

simplyRNA Tissue Kit (Promega, Leiden, the Netherlands). Slices were homogenised in homogenisation buffer using a minibead beater. The homogenate was diluted 1 : 1 with lysis buffer. The mixture was processed according to the manufacturer's protocol using the Maxwell machine. RNA concentration was quantified on a NanoDrop One UV-Vis Spectrophotometer (Thermoscientific, Wilmington, US) right before conversion to cDNA.

cDNA generation. RNA samples were diluted to 0.5 μg in 8.5 μL of RNAse free water. cDNA was generated from RNA using random primers with TaqMan Reverse Transcription Reagents Kits (Applied Biosystems, Foster City, CA). To each sample the following solutions were added: 2.5 μL 5× RT-buffer, 0.25 μL 10 mM dNTP's, 0.25 μL Rnasin (10 units), 0.5 μL M-MLV Reverse Transcriptase (100 units), 0.5 μL random primers. cDNA was generated in the Eppendorf mastercycler (Hamburg, Germany) with a gradient of 20 °C for 10 min, 42 °C for 30 min, 20 °C for 12 min, 99 °C for 5 min and finally, 20 °C for 5 min.

qRT-PCR. Real-time quantitative RT-PCR was used to determine relative mRNA levels of a set of specific genes involved in toxicity pathways. RT-PCR was performed using SensiMixTM SYBR Low-ROX kit (Bioline, London, UK) with the QuantStudio 7 Flex Real-Time PCR System (Thermoscientific, Wilmington, US) with 1 cycle of 10 min at 95 °C, 40 cycles of 15 s at 95 °C and 25 s at 60 °C, with a final dissociation stage of 15 s at 95 °C, 1 min at 60 °C and 15 s at 95 °C. cDNA for each sample was diluted to 2 ng μL^{-1} and measured in triplicate. All primers (Table 1) were purchased from Sigma-Aldrich. Fold induction of each gene was calculated using the housekeeping gene GAPDH.

Statistics

Three independent experiments (with exception of ICP-MS which was performed twice) were performed using slices in triplicates from each rat kidney or liver. The TC_{50} values were calculated as the concentration reducing the viability of the slices by 50%, relative to the untreated samples using a nonlinear fitting of log(concentration compound) *vs.* response and is presented as a mean (±SD) of at least three independent experiments. Statistical testing was performed with one-way ANOVA with each individual experiment as random effect with a Tukey HSD *post-hoc* test for pairwise comparisons. A *p*-value of ≤ 0.05 was considered to be significant. In all graphs and tables, the mean values and standard deviation (SD) are shown.

Electrospray ionization mass spectrometry (ESI-MS)

Samples were prepared by mixing 100 μM ubiquitin, (Ub, Sigma, U6253) with an excess of gold compound (300 μM) (3 : 1, metal : protein molar ratio) in 20 mM $(NH_4)_2CO_3$ buffer (pH 7.4) and incubated for 24 h at 37 °C. Prior to analysis samples were extensively ultrafiltered using a Centricon YM-3 filter (Amicon Bioseparations, Millipore Corporation) in order to remove the unbound complex. ESI-MS data were acquired on a Q-Tof Ultima mass spectrometer (Waters) fitted with a standard Z-spray ion source and operated in the positive ionization mode. Experimental parameters were set as follows: capillary voltage 3.5 kV, source temperature 80 °C, desolvation temperature 120 °C, sample cone voltage 100 V, desolvation gas flow 400 L h^{-1}, acquisition window 300–2000 *m*/*z* in 1 s. The samples were diluted 1 : 20 in water and 5 μL was introduced into the mass spectrometer by infusion at a flow rate of 20 μL min^{-1} with a solution of $CH_3CN/H_2O/HCOOH$ 50 : 49.8 : 0.2 (v : v : v). External calibration was carried out with a solution of phosphoric acid at 0.01%. Data were processed using the MassLynx 4.1 software.

Results

Viability and TC_{50}

Complexes **1–3** (Fig. 1) were tested for their possible toxicity in healthy rat kidney and liver PCTS.[6,7] Kidney and liver slices were incubated with various concentrations of each gold complex and the viability of the tissues was determined measuring the ATP content after 24 h (Fig. 2). Lansoprazole, cisplatin and auranofin were also tested for comparison. All the evaluated compounds, including cisplatin and auranofin, displayed a concentration dependent toxicity profile, with the dinuclear complex **3** and auranofin[46] as the most toxic, with a TC_{50} below 10 μM (Table 2). The ligand lansoprazole was poorly toxic in both organs. The neutral complex **2** is the least toxic of the three complexes, with TC_{50} values *ca.* 25 μM in both liver and kidney, and the lowest observed anticancer effects *in vitro*. Of note, no significant differences were found for the toxicity of complexes **1** and **2** in kidney slices, despite

Table 1 Primer sequences used in qPCR

Gene	Forward (5′-3′)	Reverse (5′-3′)
ALDOA	ACGAGGTTCTGGTGACCCTA	CCGGAGCTACAATTCGGTGA
ENO2	GTACCACACACTCAAGGGGG	TCGTATTTGCCATCGCGGTA
SLC2A1	TCAAACATGGAACCACCGCT	AGAAACCCATAAGCACGGCA
GCLM	TCAAGCTCACAACTCAGGGG	CGCCAGGGAGGTACTCAAAC
HMOX-1	CACGCATATACCCGCTACCT	AAGGCGGTCTTAGCCTCTTC
p53	CCCCTGAAGACTGGATAAC	AACTCTGCAACATCCTGGGG
BAX	ACAGGGGCCTTTTTGTTACAG	GGGGAGTCCGTGTCCACGTCA
SULF2	CGTGTGTGTTTAGAGGCGAGC	AGCCTCTTTCCGCTTTTTGGT
GAPDH	CGCTGGTGCTGAGTATGTCG	CTGTGGTCATGAGCCCTTCC

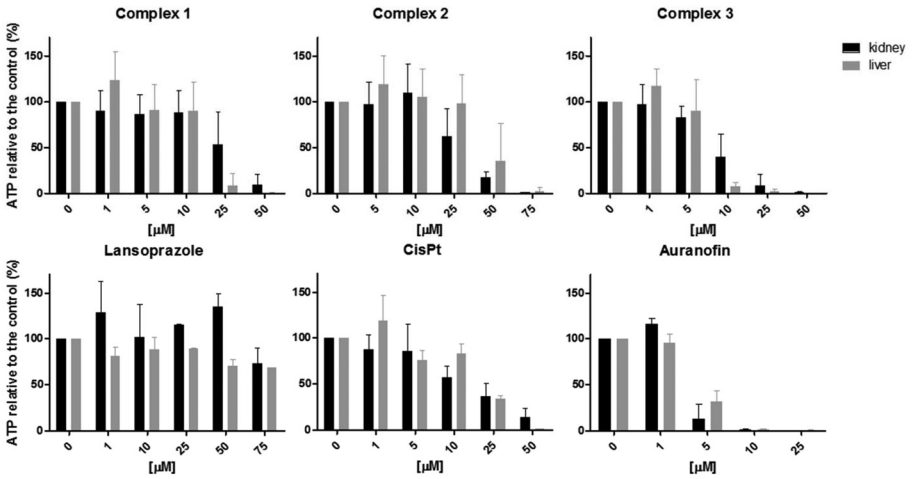

Fig. 2 Viability of rat PCKS and PCLS expressed as amount of ATP per mg protein relative to the controls (untreated slices) after treatment with complexes **1–3**, lansoprazole, cisplatin and auranofin for 24 h. The error bars show the standard deviation of three to six independent experiments.

Table 2 Toxicity of Au(I) complexes in PCKS and PCLS (TC_{50} values after 24 h incubation) and their comparison with the EC_{50} of the antiproliferative effects in cancer cell lines (72 h incubation)

	EC_{50} [a] (μM)		TC_{50} [a] (μM)		TC_{50}/EC_{50} [b]	
Compound	A2780	A2780R	Kidney	Liver	Kidney	Liver
1	1.1 ± 0.3	0.7 ± 0.1	19 ± 9	9 ± 3	27.1	12.9
2	16.2 ± 1.1	13.2 ± 4.6	25 ± 6	25 ± 3	1.9	1.9
3	1.5 ± 0.3	0.9 ± 0.4	8 ± 5	4 ± 1	8.9	4.4
Lansoprazole	45.6 ± 2.6	59.0 ± 15.2	>75	>75	NR[d]	NR[d]
Cisplatin	2.4 ± 0.6	35.0 ± 7.0*	17 ± 2	24 ± 1	0.5	0.7
Auranofin	1.25 ± 0.5[c]	1.5± 0.3[c]	3 ± 1	4 ± 1	2.0	2.7

[a] The reported values are the mean ± SD of three to six independent experiments. ND: Not determined. [b] EC_{50} of A2780R. [c] Values taken from ref. 46. [d] NR: Not relevant.

differences in their antiproliferative effects in cancer cells, while **1** was more toxic in liver slices (TC_{50} = 9 ± 3 μM).

Moreover, the mononuclear Au(I) complex **1** was two-fold less toxic than its dinuclear analogue **3** in both organs.

The obtained *ex vivo* results were further related to the cytotoxicity observed towards the previously tested cisplatin-sensitive and cisplatin-resistant cancer cells[26] (Table 2). At variance with cisplatin, the gold compounds, including auranofin, showed a similar toxicity in these two cell lines, suggesting activity *via* different mechanisms of action.[26] The safety margin for toxicity was calculated as the ratio TC_{50} PCKS/EC_{50}, where the TC_{50} is the concentration reducing the ATP content by 50% and the EC_{50} the concentration reducing the number of viable A2780R cancer cells for complex **1**, **2** and **3** and lansoprazole to 50%. In the case of complex **2** and **3** the safety margin for toxicity is poor, with values between 1.9 and 8.9. Similarly, auranofin presents a low TC_{50} PCKS/EC_{50} ratio with values between 2 and 2.7. Instead, the TC_{50} PCKS/EC_{50} cells ratio of complex **1** is *ca.* 27 for kidney, and *ca.* 13 for liver slices, indicating selective cytotoxicity towards both types of cancer cells compared to healthy tissue.

Metal content analysis

In order to assess the intracellular accumulation of the Au complexes and to evaluate the relationship between toxicity and cellular metal content, we determined the Au content in the PCKS and PCLS by ICP-MS. Additionally, the concentration of Pt was assessed in the slices exposed to cisplatin.

PCKS and PCLS were incubated with the compounds for 24 h under the same conditions as for the viability experiments. Concentrations of cisplatin and Au complexes below their TC_{50} were assessed in order to observe toxicity but guaranteeing having enough viable cells to have effective tissue accumulation. The metal content (Au or Pt) in the slices was evaluated using ICP-MS. As shown in Fig. 3, metal uptake increases significantly as a function of the concentration. In the case of cisplatin, there is a higher accumulation of Pt in the kidney tissue compared with the liver, which is in line with the results obtained in previous studies.[15]

Conversely, for all the Au(I) complexes, the Au content is higher in liver than in kidney. Interestingly, both in liver and kidney slices, the dinuclear complex **3** caused a higher

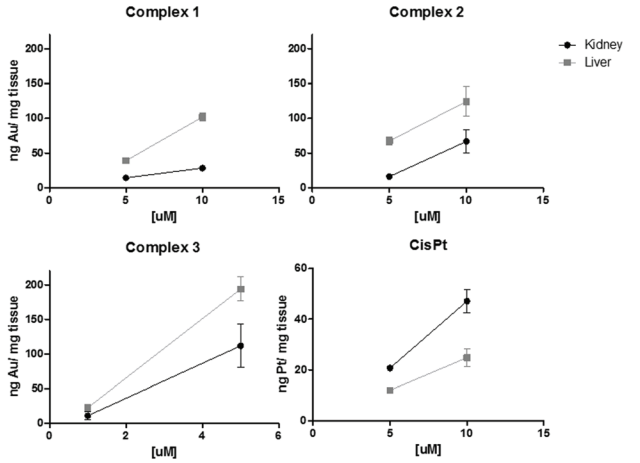

Fig. 3 Total metal content (Au or Pt) determined by ICP-MS in kidney and liver slices exposed to complexes **1–3** and cisplatin after 24 h incubation. The error bars show the standard deviation of two independent experiments.

accumulation of Au than its mononuclear analogue (complex **1**). However, the accumulation of Au for complex **3** at 5 μM is 5–8-fold higher than for complex **1** at 5 μM, which is much higher than the two-fold difference in Au content between the two complexes.

In the case of kidney slices the average metal content was 14.3 and 111.78 ng of Au per mg of tissue when treated with complex **1** and **3** (5 μM), respectively. Accordingly, in the liver slices the average metal content at 5 μM of complex **1** and **3** was 39.2 and 193.9 ng of Au per mg of tissue, respectively, although at this concentration the viability of PCLS and PCKS was not different (Fig. 2). Thus, the higher metal content in the liver slices might account for the lower TC_{50} in liver compared to kidney slices for both compounds.

Concerning the neutral Au(I) complex **2**, despite its lower toxicity (Table 2), Au uptake is comparable to complex **1** in both organs. Finally, the Pt accumulation in both tissues treated with cisplatin is always lower than the Au accumulation observed in the case of complexes **1–3**.

Histomorphology

In order to explore the localization of the damage in the different histology structures of the kidney induced by the Au compounds compared to cisplatin, morphological analysis of the PCKS was performed. The characteristic toxic effects on kidney slices of complexes **1–3**, cisplatin and auranofin were evaluated at a concentration close to the calculated TC_{50} for each compound (25 μM for complexes **1**, **2** and cisplatin; 10 μM for complex **3** and 5 μM for auranofin). Lansoprazole was not included in this evaluation because of the low toxicity observed during the viability experiments. Periodic acid-Schiff staining (PAS) was used to evaluate the integrity of the kidney slices and particularly to visualize the basement membranes and epithelial brush border in the proximal tubule cells, as reported in the Experimental section. After 24 h incubation, the untreated kidney slices show minor morphological changes, such as occasional pyknosis and swelling of some of the tubular cells (Fig. 4A). Pronounced toxic effects were observed upon treatment with complexes **1**, **2**, **3** and auranofin which induced dilatation of Bowman's space in the glomerulus and necrosis of the distal tubule cells, as well as discontinuation of the brush border in some of the proximal tubule cells (Fig. 4B–D and F). Similar toxic effects were observed in PCKS exposed to a Au(I) N-heterocyclic carbene complex, which induced similar features in the Bowman's space in the glomerulus and in the distal and proximal tubule cells.[21] In contrast, exposure of slices to cisplatin (Fig. 4E) showed injury to the proximal tubular cells with loss of nuclei and more distinct damage of the brush border; additionally, damage of the distal tubule is evident as previously reported in the literature.[16,21]

Stress markers expression

To gain insight in the specific type of stress that the Au complexes induced in this study, we studied the mRNA expression of selected specific genes that code for proteins that belong to pathways that are activated under hypoxia (Hif1a),[47] oxidative stress (Nrf2)[48] and DNA damage (p53).[49]

Based on the work of Limonciel, *et al.*,[50] we chose two or three genes related with the mentioned pathways that displayed significant up or down regulation after treating human and rat hepatocytes, and RPTEC/TERT1 cells (human renal proximal tubule cell line transfected with human telomerase) with several known toxicants.[50] Each of the selected biomarkers was expressed by kidney and liver cells. For these experiments liver and kidney slices were treated with the compounds at concentrations close to the calculated TC_{50} values (1 and 10 μM for complex **1** and **3**, 5 and 25 μM for complex **2**, 50 and 75 μM for lansoprazole) during 24 h.

From the Hif1α (hypoxia-inducible factor 1α) pathway, we selected to evaluate the expression levels of ALDOA that codes for fructose-bisphosphate aldolase A enzyme, ENO2 that codes for enolase 2, and SLC2A1 that codes for the glucose transporter protein type 1 (GLUT1). All these genes promote survival of cells in hypoxic conditions by inducing glycolysis.[47] In the case of PCKS no significant up or down regulation of any of the selected genes was observed (Fig. 5), indicating that the compounds do not promote a hypoxic environment as a toxicity mechanism. In the case of PCLS, the responses were more diverse, where exposure of PCLS to complex **1** seemed to induce an upregulation of SLC2A1 gene at the highest concentration only.

Moreover, treatment with complex **3** at 10 μM induced upregulation of *ca.* 3-fold of ENO2 compared with the untreated samples. These results suggest some activation of the hypoxia pathway in the liver slices. Lansoprazole did not induce any change in the expression of the tested genes. Further experiments are necessary to fully understand if activation of the hypoxia pathway is the main cause of toxicity, specifically in the case of liver tissue, using different bio-markers, such as Hif1α and FABP3 (fatty acid binding protein 3).[47,51]

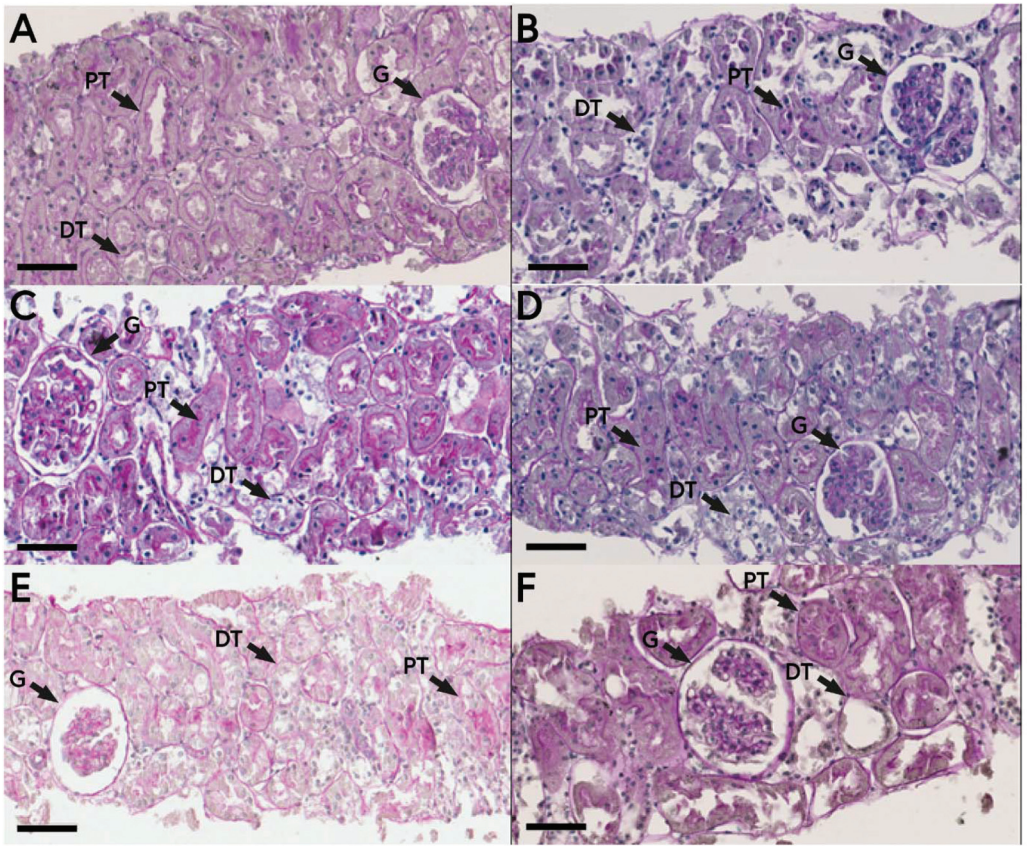

Fig. 4 Morphology of rat kidney slices. A: 24 h control incubation; B: complex **1** (25 μM); C: complex **2** (25 μM); D: complex **3** (10 μM); E: cisplatin (25 μM) and F: auranofin (5 μM). PT: proximal tubule, DT: distal tubule, G: glomerulus. Scale bar indicates 50 μm.

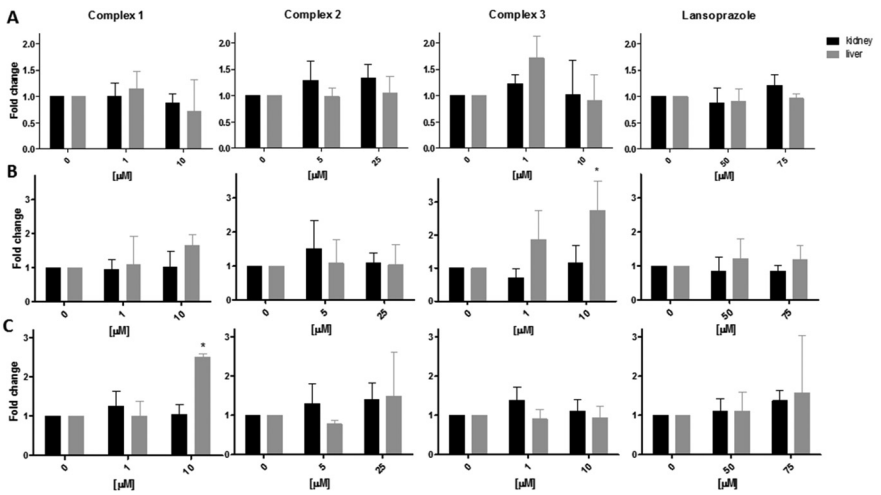

Fig. 5 Gene expression of ALDOA (A), ENO2 (B) and SLC2A1 (C) in kidney (black bars) and liver slices (grey bars) exposed to complexes **1**, **2**, **3** and lansoprazole for 24 h, in comparison to untreated slices set as 1. The error bars show the standard deviation of three independent experiments. Statistical significance ($p < 0.05$) is shown as *.

The selected genes from the Nrf2 pathway include GCLM and HMOX-1. GCLM codes for glutamate-cysteine ligase modifier subunit of glutamate-cysteine ligase and is the first and rate-limiting step enzyme of the glutathione biosynthetic pathway.[52] HMOX-1 codes for heme oxygenase 1, which is an essential enzyme in heme catabolism and plays an important role as antioxidant under oxidative stress conditions.[53] Both genes are overexpressed under oxidative stress conditions in

kidney and liver tissue to detoxify the excessive production of free radicals.[54–56] GLCM expression was significantly upregulated by the higher concentration of complex **3** in kidney slices, whereas in liver slices the effect was not evident. HMOX-1 expression was also significantly upregulated by the higher concentration of complex **3** in kidney and liver slices. A trend towards upregulation of HMOX-1 was observed after treatment of PCKS and PCLS with complexes **1** and **2**; although the differences are not significant in all cases, an analysis of the individual experiments revealed a trend towards upregulation of both genes (Fig. 6). Furthermore, lansoprazole did not induce any change in the expression of the tested genes. Additional experiments evaluating the glutathione and thioredoxin intracellular redox balance could lead to confirmation of our findings.

The p53 pathway was also explored by determining the expression levels of protein p53. Protein p53 stimulates the expression of a set of arrest-upon-cellular-stress signals induced by DNA damage, downstream target genes that are involved in induction of apoptosis, facilitation of DNA repair or activation of cell cycle oncogene activation and hypoxia.[57–60] BAX codes for the Bcl-2-enzyme sulfatase 2, which is upregulated upon activation of p53 due to DNA damage, thereby affecting the cell cycle.[61] Neither p53, BAX or SULF-2 showed major regulation changes upon treatment of kidney and liver slices by any of the tested compounds (Fig. 7). These findings are in line with the lack of caspase 3 and 7 activation observed in PCKS (data not shown), indicating that apoptosis *via* DNA damage is not the mechanism of gold compounds' induced cell death in tissue slices. Conversely, cisplatin covalently

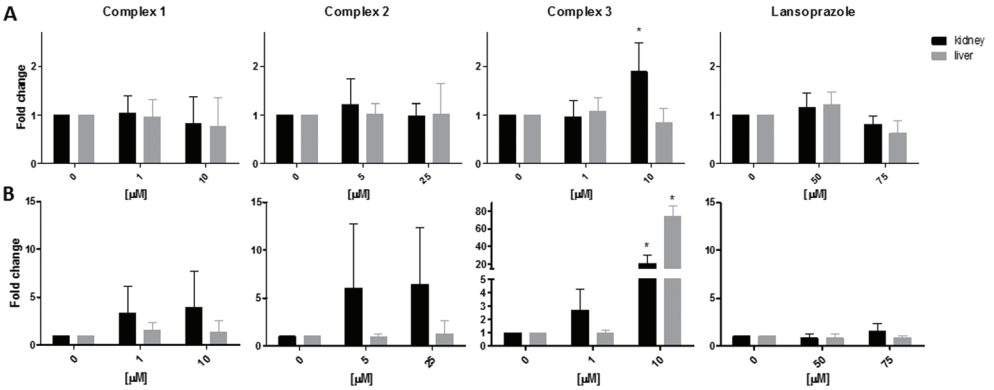

Fig. 6 Gene expression of GCLM (A) and HMOX-1 (B) in kidney and liver slices exposed to complexes **1**, **2**, **3** and lansoprazole for 24 h, in comparison to untreated slices set as 1. The error bars show the standard deviation of three independent experiments. Statistical significance ($p < 0.05$) is shown as *.

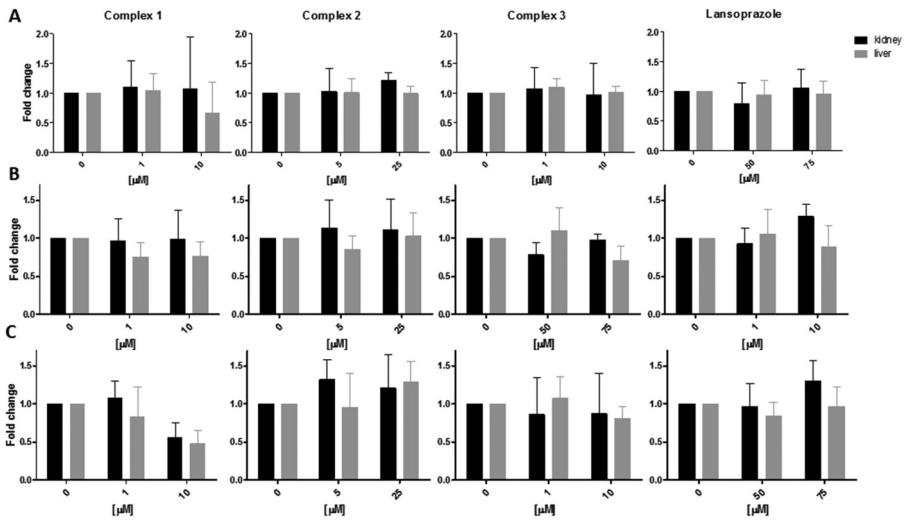

Fig. 7 Gene expression of p53 (A), BAX (B) and SULF-2 (C) in kidney and liver slices exposed to complexes **1**, **2**, **3** and lansoprazole for 24 h, in comparison to untreated slices set as 1. The error bars show the standard deviation of three independent experiments. Statistical significance ($p < 0.05$) is shown as *.

binds DNA nucleobases leading to apoptosis as the main mechanism of toxicity, with marked upregulation of p53 and BAX.[62–64]

Reactivity with model protein ubiquitin

In order to shed light on the reactivity of the Au complexes we investigated their interactions with ubiquitin (Ub), used as a model protein, by electrospray ionization mass spectrometry (ESI-MS) following established protocols.[46,65,66] Ub is a small tightly folded protein of 76 amino acids which has several potential binding sites for metal centers, including a Met residue with high affinity for Au binding.[66] Thus, three molar equivalents of complexes **1** and **2** were added to an aqueous solution of Ub buffered at pH 7.4 (see Experimental for details). Fig. S1† in the supplementary material shows the mass spectra of the Ub-**1** and Ub-**2** samples recorded after 24 h incubation. In the spectrum, Ub was identified as one of the main peaks at 952.65 *m*/*z* (charge state +9, *ca.* 8565 Da), and gold-containing species were observed at 974.45 *m*/*z* (charge state +9, *ca.* 197 Da) corresponding to an Ub–Au adduct in which the original lansoprazole ligand is absent. The observed reactivity is similar to the one described for the reference compound auranofin[67] and similar Au(I) complexes.[46]

Discussion and conclusions

The potential therapeutic application of lansoprazole Au(I) complexes with antiproliferative effects[26] prompted us to study their toxicity in healthy tissue using kidney and liver slices, aiming to predict the possible side effects when the complexes are administered *in vivo*. Thus, the toxicity was evaluated by measuring the ATP content as well as by histomorphology and metal content analysis by ICP-MS, in PCTS. Additionally, mRNA expression of specific stress markers was assessed in tissue slices, including expression of genes coding for proteins that play important roles in pathways of oxidative stress, apoptosis and hypoxia. The obtained ATP results showed a different toxicity profile for the tested compounds. The neutral complex **2** shows the lowest toxicity in both liver and kidney slices, also lower than cisplatin, followed by the cationic complex **1**, whereas the dinuclear and cationic complex **3** is the most toxic in the liver and kidney slices. Notably, both complexes **1** and **3** bear triphenylphosphine ligands, known to be intrinsically toxic,[34] while the PTA (1,3,5-triaza-7-phosphaadamantane) ligand of complex **2** is non-toxic. As expected, in kidney and liver slices complex **1** (with one phosphine ligand and one Au ion) is less toxic than the dinuclear diphosphane complex **3**. However, as the amount of Au taken up was reasonably well in line with the toxicity, based on the TC_{50} *via* ATP determination, the higher Au uptake of **3**, combined to the phosphine activity, may be mainly responsible for the higher toxicity.

Considering that the selectivity of a compound for cancer cells compared to healthy organs is the most relevant parameter when selecting it for further preclinical trials, the ratio of the TC_{50} in slices to the EC_{50} in the cisplatin-resistant cancer cells was calculated for each gold compound. Using this parameter, complex **1** presents the best ratio of toxicity in healthy tissue to anticancer efficacy when compared to the other tested complexes. This ratio is also much higher for complex **1** than for cisplatin, which may indicate that this compound can lead to a promising drug candidate for further development. However, it should be stressed that these ratios do not represent the absolute values of selectivity, because the cancer cell lines model and the tissue slices are different. Nevertheless, the calculated ratios can be used to compare the different compounds with standard anticancer drugs like cisplatin.

Furthermore, the histomorphology evaluation shows similarities for all three Au(I) complexes with respect to the specific kidney cell types that suffer the most extensive damage, as they seem to be preferentially toxic towards the distal tubular cells. This result is in contrast to cisplatin, which is known to show toxicity mainly in the proximal tubular cells as described in previous reports.[16,21,22]

ICP-MS data on PCTS treated with the Au(I) complexes show that in all cases the Au content is higher in the liver PCTS than in the kidney PCTS, at variance with the Pt content for cisplatin treated slices. Nevertheless, marked differences in the uptake and extent of cellular damage of the Au complexes were also observed, particularly considering the efficient Au accumulation for the dinuclear cationic derivative **3**. It is also worth mentioning that, despite the lower toxicity of complex **2** compared to cisplatin in PCTS, the Au content in the slices was higher than the Pt content as shown by ICP-MS. The observed toxic effects may also depend on the accumulation of the compounds in specific cell types. Overall, these results corroborate the idea of different mechanisms of tissue accumulation and sub-cellular localization of the tested metallodrugs.[68] The fact that the Au(I) complex **2** is neutral, and the other two, **1** and **3** positively charged, may well differentiate its uptake and cellular localization.

In terms of the possible reactivity, it should be noted that previous studies on Au(I) complexes with N-donor and phosphine ligands have evidenced that these compounds are prone to ligand exchange processes upon reaction with intracellular proteins/enzymes (*e.g. via* binding to Cys and Met residues).[46,66,69] According to these results, upon thiol and thioether binding, the Au(I) complexes release their ligands and the 'free' gold ions remain bound to the amino acid side chains. In addition, further reduction of Au(I) to Au(0) upon protein binding cannot be excluded. In this study, the ESI-MS results confirm the lansoprazole and phosphine ligands' loss upon binding to the model protein ubiquitin of compounds **1** and **2**.

Interestingly, based on the gene expression data, of all the stress pathways evaluated, the clearest impact of the compounds' administration was on the Nrf2 pathway, indicating oxidative stress as a possible mechanism of toxicity. Instead, no indication of apoptosis induction *via* DNA binding and upregulation of p53 and BAX was observed, at variance with cisplatin. This result is in line with previously reported data,

according to which Au(I) complexes cause the inhibition of the seleno-enzyme thioredoxin reductase (TrxR) involved in the maintenance of the intracellular redox balance.[70,71] In future studies, it might be relevant to include specific markers for distinct cell types in the kidney and the liver to get more information about the cell-specific toxicity of the compounds evaluated in this study.

The obtained results open new perspectives towards the understanding of the selectivity and mechanism of toxicity of the lansoprazole-based Au(I) complexes and prompt us to pursue the design of new families of anticancer bifunctional gold compounds, with reduced toxicity in healthy tissues.

Conflicts of interest

There are no conflicts of interest to declare.

Acknowledgements

The authors thank the Department of Sciences, Technology, and Innovation COLCIENCIAS (Colombia) for a PhD fellowship to N.E.O. Eduard Post and Marina de Jager are acknowledged for assistance during the *ex vivo* experiments.

References

1 Y. Imamura, T. Mukohara, Y. Shimono, Y. Funakoshi, N. Chayahara, M. Toyoda, N. Kiyota, S. Takao, S. Kono, T. Nakatsura and H. Minami, *Oncol. Rep.*, 2015, **33**, 1837–1843.
2 V. Ahuja, S. Bokan and S. Sharma, *Drug Discovery Today*, 2017, **22**, 127–132.
3 H. Attarwala, *J. Young Pharm.*, 2010, **2**, 332–336.
4 D. Butler and E. Callaway, *Nat. News*, 2016, **529**, 263.
5 J. Kimmelman and C. Federico, *Nat. News*, 2017, **542**, 25.
6 I. A. M. de Graaf, G. M. Groothuis and P. Olinga, *Expert Opin. Drug Metab. Toxicol.*, 2007, **3**, 879–898.
7 I. A. M. de Graaf, P. Olinga, M. H. de Jager, M. T. Merema, R. de Kanter, E. G. van de Kerkhof and G. M. M. Groothuis, *Nat. Protoc.*, 2010, **5**, 1540–1551.
8 A. E. M. Vickers and R. L. Fisher, *Xenobiotica*, 2013, **43**, 29–40.
9 A. Wolf, A. Vickers, P. Olinga, A. Braun, C. Martin, G. Groothuis and N. Shangari, *Toxicol. Suppl. Toxicol. Sci.*, 2011, **120**, 379–379.
10 G. M. M. Groothuis, A. Casini, H. Meurs and P. Olinga, *Human-based Systems for Translational Research*, 2014, pp. 38–65.
11 F. Poosti, B. T. Pham, D. Oosterhuis, K. Poelstra, H. van Goor, P. Olinga and J.-L. Hillebrands, *Dis. Models Mech.*, 2015, **8**, 1227–1236.
12 I. M. Westra, D. Oosterhuis, G. M. M. Groothuis and P. Olinga, *Toxicol. Appl. Pharmacol.*, 2014, **274**, 328–338.
13 I. M. Westra, H. A. M. Mutsaers, T. Luangmonkong, M. Hadi, D. Oosterhuis, K. P. de Jong, G. M. M. Groothuis and P. Olinga, *Toxicol. in Vitro*, 2016, **35**, 77–85.
14 P. Olinga and D. Schuppan, *J. Hepatol.*, 2013, **58**, 1252–1253.
15 J. Han, A. F. B. Räder, F. Reichart, B. Aikman, M. N. Wenzel, B. Woods, M. Weinmüller, B. S. Ludwig, S. Stürup, G. M. M. Groothuis, H. P. Permentier, R. Bischoff, H. Kessler, P. Horvatovich and A. Casini, *Bioconjugate Chem.*, 2018, **29**, 3856–3865.
16 A. E. M. Vickers, K. Rose, R. Fisher, M. Saulnier, P. Sahota and P. Bentley, *Toxicol. Pathol.*, 2004, **32**, 577–590.
17 A. R. Parrish, A. J. Gandolfi and K. Brendel, *Life Sci.*, 1995, **57**, 1887–1901.
18 B. Bertrand, L. Stefan, M. Pirrotta, D. Monchaud, E. Bodio, P. Richard, P. Le Gendre, E. Warmerdam, M. H. de Jager, G. M. M. Groothuis, M. Picquet and A. Casini, *Inorg. Chem.*, 2014, **53**, 2296–2303.
19 B. Bertrand, A. Citta, I. L. Franken, M. Picquet, A. Folda, V. Scalcon, M. P. Rigobello, P. Le Gendre, A. Casini and E. Bodio, *J. Biol. Inorg. Chem.*, 2015, **20**, 1005–1020.
20 J. K. Muenzner, T. Rehm, B. Biersack, A. Casini, I. A. M. de Graaf, P. Worawutputtapong, A. Noor, R. Kempe, V. Brabec, J. Kasparkova and R. Schobert, *J. Med. Chem.*, 2015, **58**, 6283–6292.
21 N. Estrada-Ortiz, F. Guarra, I. A. M. de Graaf, L. Marchetti, M. H. de Jager, G. M. M. Groothuis, C. Gabbiani and A. Casini, *ChemMedChem*, 2017, **12**, 1429–1435.
22 S. Spreckelmeyer, N. Estrada-Ortiz, G. G. H. Prins, M. van der Zee, B. Gammelgaard, S. Stürup, I. A. M. de Graaf, G. M. M. Groothuis and A. Casini, *Metallomics*, 2017, **9**, 1786–1795.
23 S. Daum, V. F. Chekhun, I. N. Todor, N. Y. Lukianova, Y. V. Shvets, L. Sellner, K. Putzker, J. Lewis, T. Zenz, I. A. M. de Graaf, G. M. M. Groothuis, A. Casini, O. Zozulia, F. Hampel and A. Mokhir, *J. Med. Chem.*, 2015, **58**, 2015–2024.
24 R. Rajaratnam, E. K. Martin, M. Dörr, K. Harms, A. Casini and E. Meggers, *Inorg. Chem.*, 2015, **54**, 8111–8120.
25 A. Schmidt, V. Molano, M. Hollering, A. Pöthig, A. Casini and F. E. Kühn, *Chemistry*, 2016, **22**, 2253–2256.
26 M. Serratice, B. Bertrand, E. F. J. Janssen, E. Hemelt, A. Zucca, F. Cocco, M. A. Cinellu and A. Casini, *Med. Chem. Commun.*, 2014, **5**, 1418–1422.
27 M. G. Apps, E. H. Y. Choi and N. J. Wheate, *Endocr.-Relat. Cancer*, 2015, **22**, R219–R233.
28 P. M. Bruno, Y. Liu, G. Y. Park, J. Murai, C. E. Koch, T. J. Eisen, J. R. Pritchard, Y. Pommier, S. J. Lippard and M. T. Hemann, *Nat. Med.*, 2017, **23**, 461–471.
29 D. Gaynor and D. M. Griffith, *Dalton Trans.*, 2012, **41**, 13239–13257.
30 P. C. A. Bruijnincx and P. J. Sadler, *Curr. Opin. Chem. Biol.*, 2008, **12**, 197–206.
31 S. J. Berners-Price and A. Filipovska, *Metallomics*, 2011, **3**, 863–873.
32 B. Bertrand and A. Casini, *Dalton Trans.*, 2014, **43**, 4209–4219.

33 K. D. Mjos and C. Orvig, *Chem. Rev.*, 2014, **114**, 4540–4563.
34 S. Nobili, E. Mini, I. Landini, C. Gabbiani, A. Casini and L. Messori, *Med. Res. Rev.*, 2010, **30**, 550–580.
35 C. Nardon, G. Boscutti and D. Fregona, *Anticancer Res.*, 2014, **34**, 487–492.
36 C. Roder and M. J. Thomson, *Drugs R&D*, 2015, **15**, 13–20.
37 D. A. Gremse, *Expert Opin. Pharmacother.*, 2001, **2**, 1663–1670.
38 T. Miyashita, F. A. Shah, J. W. Harmon, G. P. Marti, D. Matsui, K. Okamoto, I. Makino, H. Hayashi, K. Oyama, H. Nakagawara, H. Tajima, H. Fujita, H. Takamura, M. Murakami, I. Ninomiya, H. Kitagawa, S. Fushida, T. Fujimura and T. Ohta, *Surg. Today*, 2013, **43**, 831–837.
39 M. Yu, C. Lee, M. Wang and I. F. Tannock, *Cancer Sci.*, 2015, **106**, 1438–1447.
40 J. M. Shin and N. Kim, *J. Neurogastroenterol. Motil.*, 2013, **19**, 25–35.
41 Z.-N. Lu, B. Tian and X.-L. Guo, *Cancer Chemother. Pharmacol.*, 2017, **80**, 925–937.
42 E. Spugnini and S. Fais, *Semin. Cancer Biol.*, 2007, **43**, 111–118.
43 J. Barar and Y. Omidi, *BioImpacts*, 2013, **3**, 149–162.
44 T. Azzarito, G. Venturi, A. Cesolini and S. Fais, *Cancer Lett.*, 2015, **356**, 697–703.
45 E. P. Spugnini, P. Sonveaux, C. Stock, M. Perez-Sayans, A. De Milito, S. Avnet, A. G. Garcìa, S. Harguindey and S. Fais, *Biochim. Biophys. Acta, Biomembr.*, 2015, **1848**, 2715–2726.
46 M. Serratrice, F. Edafe, F. Mendes, R. Scopelliti, S. M. Zakeeruddin, M. Grätzel, I. Santos, M. A. Cinellu and A. Casini, *Dalton Trans.*, 2012, **41**, 3287–3293.
47 G. L. Semenza, *Sci. STKE*, 2007, **2007**, cm8.
48 Q. Ma, *Annu. Rev. Pharmacol. Toxicol.*, 2013, **53**, 401–426.
49 D. P. Lane, *Nature*, 1992, **358**, 15–16.
50 A. Limonciel, K. Moenks, S. Stanzel, G. L. Truisi, C. Parmentier, L. Aschauer, A. Wilmes, L. Richert, P. Hewitt, S. O. Mueller, A. Lukas, A. Kopp-Schneider, M. O. Leonard and P. Jennings, *Toxicol. in Vitro*, 2015, **30**, 7–18.
51 T. Biron-Shental, W. T. Schaiff, C. K. Ratajczak, I. Bildirici, D. M. Nelson and Y. Sadovsky, *Am. J. Obstet. Gynecol.*, 2007, **197**, 516.e1-6.
52 S. C. Lu, *Mol. Aspects Med.*, 2009, **30**, 42–59.
53 V. Calabrese, A. Signorile, C. Cornelius, C. Mancuso, G. Scapagnini, B. Ventimiglia, N. Ragusa and A. Dinkova-Kostova, in *Methods in Enzymology*, ed. E. Cadenas and L. Packer, Academic Press, 2008, vol. 441, pp. 83–110.
54 M.-L. Cheng, Y.-F. Lu, H. Chen, Z.-Y. Shen and J. Liu, *Hepatobiliary Pancreatic Dis. Int.*, 2015, **14**, 485–491.
55 R. K. Zalups and D. J. Koropatnick, *Cellular and Molecular Biology of Metals*, CRC Press, 2010.
56 K. A. Nath, J. P. Grande, J. J. Haggard, A. J. Croatt, Z. S. Katusic, A. Solovey and R. P. Hebbel, *Am. J. Pathol.*, 2001, **158**, 893–903.
57 A. Vazquez, E. E. Bond, A. J. Levine and G. L. Bond, *Nat. Rev. Drug Discovery*, 2008, **7**, 979–987.
58 J. S. Fridman and S. W. Lowe, *Oncogene*, 2003, **22**, 9030–9040.
59 S. Sengupta and C. C. Harris, *Nat. Rev. Mol. Cell Biol.*, 2005, **6**, 44–55.
60 L. E. Giono and J. J. Manfredi, *J. Cell. Physiol.*, 2006, **209**, 13–20.
61 S. D. Rosen and H. Lemjabbar-Alaoui, *Expert Opin. Ther. Targets*, 2010, **14**, 935–949.
62 S. Dasari and P. B. Tchounwou, *Eur. J. Pharmacol.*, 2014, 364–378.
63 J.-Y. Han, Y.-J. Chung, S. W. Park, J. S. Kim, M.-G. Rhyu, H.-K. Kim and K. S. Lee, *Korean J. Intern. Med.*, 1999, **14**, 42–52.
64 A. di Pietro, R. Koster, W. Boersma-van Eck, W. A. Dam, N. H. Mulder, J. A. Gietema, E. G. E. de Vries and S. de Jong, *Cell Cycle*, 2012, **11**, 4552–4562.
65 M. Wenzel, B. Bertrand, M.-J. Eymin, V. Comte, J. A. Harvey, P. Richard, M. Groessl, O. Zava, H. Amrouche, P. D. Harvey, P. Le Gendre, M. Picquet and A. Casini, *Inorg. Chem.*, 2011, **50**, 9472–9480.
66 M. Wenzel and A. Casini, *Coord. Chem. Rev.*, 2017, **352**, 432–460.
67 J. R. Roberts, J. Xiao, B. Schliesman, D. J. Parsons and C. F. Shaw, *Inorg. Chem.*, 1996, **35**, 424–433.
68 S. Spreckelmeyer, C. Orvig and A. Casini, *Molecules*, 2014, **19**, 15584–15610.
69 L. Mazzei, M. N. Wenzel, M. Cianci, M. Palombo, A. Casini and S. Ciurli, *ACS Med. Chem. Lett.*, 2019, **10**, 564–570.
70 A. Bindoli, M. P. Rigobello, G. Scutari, C. Gabbiani, A. Casini and L. Messori, *Coord. Chem. Rev.*, 2009, **253**, 1692–1707.
71 A. Casini, C. Gabbiani, F. Sorrentino, M. P. Rigobello, A. Bindoli, T. J. Geldbach, A. Marrone, N. Re, C. G. Hartinger, P. J. Dyson and L. Messori, *J. Med. Chem.*, 2008, **51**, 6773–6781.